ENVIRONMENTAL RESEARCH
LETTERS

LETTER • OPEN ACCESS

Increasing tropical cyclone intensity and potential intensity in the subtropical Atlantic around Bermuda from an ocean heat content perspective 1955–2019

To cite this article: Samantha Hallam *et al* 2021 *Environ. Res. Lett.* **16** 034052

ENVIRONMENTAL RESEARCH
LETTERS

OPEN ACCESS

RECEIVED
21 August 2020

REVISED
9 February 2021

ACCEPTED FOR PUBLICATION
9 February 2021

PUBLISHED
2 March 2021

LETTER

Increasing tropical cyclone intensity and potential intensity in the subtropical Atlantic around Bermuda from an ocean heat content perspective 1955–2019

Samantha Hallam[1,2], **Mark Guishard**[3,4], **Simon A Josey**[1], **Pat Hyder**[5] **and Joel Hirschi**[1]

[1] National Oceanography Centre, European Way, Southampton SO14 3ZH, United Kingdom
[2] University of Southampton, National Oceanography Centre, European Way, Southampton SO14 3ZH, United Kingdom
[3] Bermuda Institute of Ocean Sciences, 17 Biological Station, St. George's GE 01, Bermuda
[4] Bermuda Weather Service, Bermuda Airport Authority, St. George's DD03, Bermuda
[5] Met Office, Fitzroy Road, Exeter EX1 3PB, United Kingdom

E-mail: s.hallam@noc.soton.ac.uk

Keywords: tropical cyclone, ocean heat content, subtropical Atlantic, Bermuda, potential intensity, Hydrostation S time-series

Supplementary material for this article is available online

Abstract

We investigate tropical cyclone (TC) activity and intensity within a 100 km radius of Bermuda between 1955 and 2019. The results show a more easterly genesis over time and significant increasing trends in TC intensity (maximum wind speed (Vmax)) with a decadal Vmax median value increase of 30 kts from 33 to 63 kts ($r = 0.94$, $p = 0.02$), together with significant increasing August, September, October sea surface temperature (SST) of 1.1 °C (0.17 °C per decade) $r = 0.4$ ($p < 0.01$) and increasing average ocean temperature between 0.5 °C and 0.7 °C (0.08 °C–0.1 °C per decade) $r = 0.3 (p < 0.01)$ in the depth range 0–300 m. The strongest correlation is found between TC intensity and ocean temperature averaged through the top 50 m ocean layer ($\overline{T_{50\,\mathrm{m}}}$) $r = 0.37$ ($p < 0.01$). We show how TC potential intensity (PI) estimates are closer to actual intensity by using $\overline{T_{50\,\mathrm{m}}}$ as opposed to SST using the Hydrostation S time-series. We modify the widely used SST PI index by using $\overline{T_{50\,\mathrm{m}}}$ to provide a closer estimate of the observed minimum sea level pressure (MSLP), and associated Vmax than by using SST, creating a $\overline{T_{50\,\mathrm{m}}}$ PI ($\overline{T_{50\,\mathrm{m}}}$_PI) index. The average MSLP difference is reduced by 12 mb and proportional ($r = 0.74$, $p < 0.01$) to the SST/$\overline{T_{50\,\mathrm{m}}}$ temperature difference. We also suggest the index could be used over a wider area of the subtropical/tropical Atlantic where there is a shallow mixed layer depth.

1. Introduction

In September 2019 Hurricane Humberto was the latest category 3 hurricane to impact Bermuda, with 100 knot winds and causing power outage to over 80% of the island, and there have been several other intense hurricanes impacting the island in the recent past: Fabian (2003), Gonzalo (2014), Nicole (2016) and Paulette (2020).

Observed Atlantic hurricane frequency has been found to correlate with the variability of sea surface temperatures (SSTs) on seasonal (Hallam *et al* 2019) to multidecadal timescales, particularly as measured by the Atlantic multi-decadal variability (AMV) index (Goldenberg *et al* 2001), which is the North Atlantic area-averaged (0–60° N, 0–80° W) sea surface temperature anomaly (SSTA). Greater hurricane frequency during warm years of the AMV is also likely due to reduced vertical wind shear and lower sea-level pressure patterns, which are correlated with positive SSTA (through greater ocean-air heat fluxes) (Klotzbach 2007). As hurricanes intensify by extracting energy from the warm ocean surface via air-sea sensible and latent heat fluxes, the underlying SSTs and upper ocean thermal structure are critical for their development and intensification (Emanuel 1987, 1999, Shay *et al* 2000, Mainelli *et al* 2008, Lloyd and Vecchi 2011, Huang *et al* 2015, Domingues *et al* 2019). When a tropical cyclone (TC) intensifies the SST reduces through surface cooling by evaporation and associated convection, vertical mixing and upwelling of cooler subsurface water. Price (2009)

find that the depth averaged ocean temperature preceding the passage of the TC, averaged from the surface to the expected cyclone induced mixing depth, is a good indication of SST during TC intensification and better reflects the layer which supplies the heat for evaporation. How the initial upper ocean thermal profile impacts on intensification is also a function of TC intensity, translation speed and size, sometimes referred as ocean coupling effect (Lloyd and Vecchi 2011, Huang *et al* 2015). Other studies have found rising SSTs increase TC maximum potential intensity (PI) (Emanuel 1987, Webster *et al* 2005, Villarini and Vecchi 2013) and positive ocean heat content (OHC) anomalies increase the hurricane intensity and track length (Mainelli *et al* 2008, Lin *et al* 2014, Balaguru *et al* 2018, Trenberth *et al* 2018).

TC intensity, defined by the minimum sea level pressure (MSLP) at the TC centre and the maximum sustained wind speed (MSW) at 10 m, can be affected by internal physical processes and the storm's interaction with the environment. Although predicting individual TC intensity remains difficult, it is accepted that thermodynamic limits to intensity exist, provided that there is no negative interaction between a storm and its environment (Emanuel 1999). Limit calculations (PI) are fairly straightforward as they are based on SST and the vertical structure of the atmosphere (Emanuel 1995). The upper limit is based on the maximum heat input from the ocean to the atmosphere and the thermodynamic efficiency related to the difference between the SST and the temperature at the level of neutral buoyancy. While PI is a good predictor of TC maximum intensity, it is a poor predictor of actual TC intensity as most TCs fail to obtain intensities near their PI (Wang and Wu (2004), Bender *et al* (2007), Lin *et al* (2013)). Bender *et al* (2007) found upper ocean coupling significantly improved TC intensity predictions measured by MSLP. Here we use the widely accepted PI estimate based on SST (SST_PI, Emanuel 1999) but also adapt it to create an average ocean temperature PI index based on initial ocean temperature through the top 50 m layer, to estimate TC $\overline{T_{50\,\mathrm{m}}}$_PI.

Oceanographic measurements from the Hydrostation S time-series (Michaels and Knap 1996, Phillips and Joyce 2007), TC data from HURDAT2 (Landsea and Franklin 2013) and atmospheric radiosonde soundings from the Bermuda Weather Service are used to investigate the TC activity and intensity around Bermuda for the period 1880–2019. GODAS ocean re-analysis data (Behringer *et al* 1998) provide SST and sub surface temperatures for the wider North Atlantic.

2. Data and methodology

TCs were analysed within a radius of 100 km from Bermuda with a search centre at 32.4° N and 64.8° W, on the basis the storms could impact Bermuda (Bell and Ray 2004). The observed Atlantic TC and hurricane track data for the years 1880–2019 were obtained from HURDAT2, the revised Atlantic hurricane database (Landsea and Franklin 2013). The data includes 6 hourly information on location, MSLP and MSW, although data availability is more limited in the early part of the record. In the data interpretation we are mindful that in the presatellite era (between 1878 and 1965) an upward adjustment of hurricane counts (and associated intensity adjustment) may be needed due to the sparse density of reporting ship traffic (Vecchi and Knutson 2011).

The Hydrostation S Time-series Site is located in the oligotrophic northern Sargasso Sea gyre about 26 km southeast of the island of Bermuda (32° 10′ N, 64° 30′ W) and provides hydrographic parameters since 1954. We use the surface and sub surface temperature profiles (0–300 m), which are collected on a biweekly to monthly basis, to calculate surface temperature and $\overline{T_{\mathrm{n}}}$ (average ocean temperature over the depth) for the period. For each TC, the temperature and depth data were obtained from conductivity, temperature and depth instruments preceding its passage into the Bermuda area, which ranged from 1 to 33 d.

TC maximum PI based on SST, which provides an estimate of the theoretical upper limit of TC intensity, was calculated based on the method and code (http://emanuel.mit.edu/products) developed by Emanuel (1999) which uses the energy cycle of the storm to estimate the maximum possible surface wind speed and also the minimum central pressure. It can be written in convective available potential energy (CAPE) terms (Emanuel 1994, Bister and Emanuel 2002)

$$V^2 = \frac{C_{\mathrm{k}}}{C_{\mathrm{D}}}\frac{T_{\mathrm{s}}}{T_0}(\mathrm{CAPE}^* - \mathrm{CAPE}) \qquad (1)$$

where V is the maximum surface wind speed, C_{k} and C_{D} are the exchange coefficients for enthalpy and drag, T_{s} and T_0 are the temperatures at the sea surface and mean outflow temperature, CAPE* is the CAPE of air lifted from saturation at sea level in reference to the environmental sounding, and CAPE represents the sounding at the radius of the maximum winds. A positive difference (CAPE* − CAPE) indicates a significant air-sea enthalpy flux into the atmosphere (mostly driven by latent heat flux) and is the environment required to assist TC maintenance.

In the evaluation of (1) the surface pressure at the radius of the maximum winds is calculated to provide the saturation mixing ratio necessary for CAPE* using equation (6) of Emanuel (1995)

$$c_{\mathrm{p}}T_{\mathrm{s}}\ln\frac{p_0}{p_{\mathrm{m}}} = \frac{1}{2}V^2 + \mathrm{CAPE}. \qquad (2)$$

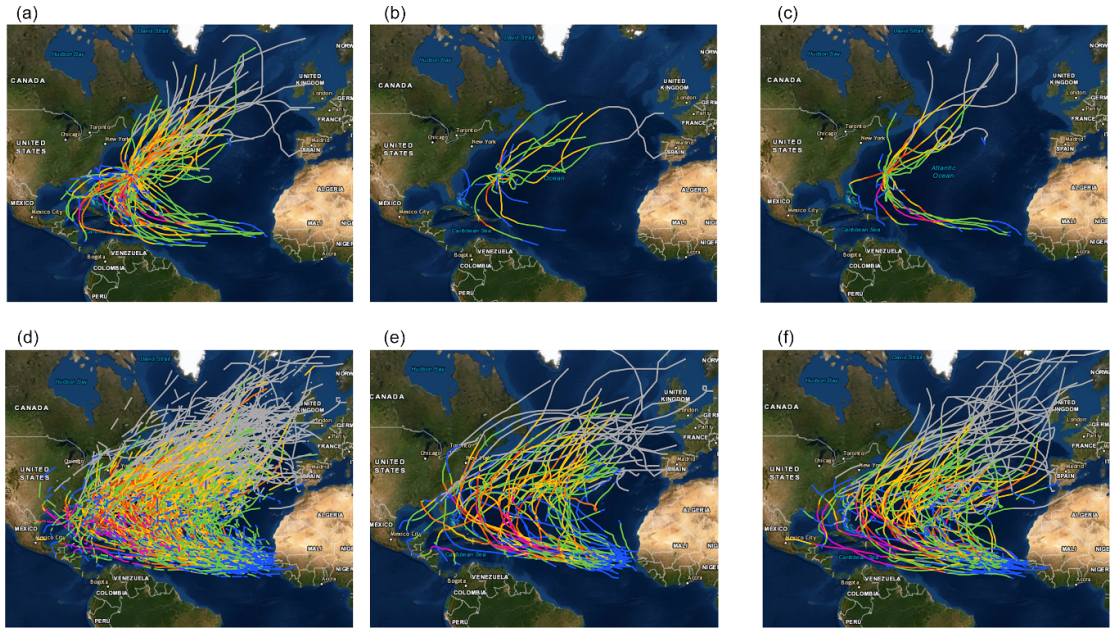

Figure 1. Tropical cyclone tracks within 100 km of Bermuda. (a) 1880–2019, (b) 1980–1999 and (c) 2000–2019. Atlantic tropical cyclone tracks (d) 1880–2019 (e) 1980–1999 and (f) 2000–2019.

c_p is the heat capacity at constant pressure, p_0 is the ambient surface pressure and p_m is the surface pressure at the radius of the maximum winds. CAPE is calculated using the mixing ratio and vertical temperature profile. Radiosonde soundings from the Bermuda Weather Service Station at LF Wade International Airport (WMO station identifier code 78016), were used to provide the vertical temperature profile and mixing ratio data. The atmospheric profiles preceded the passage of the storm to represent the undisturbed environment (Emanuel *et al* 2004). For comparison to the PI estimates, actual V and minimum central pressure of the TC were taken from the HURDAT2 data.

3. Results

3.1. Hurricane season activity and intensity

There were 93 TC tracks which passed within 100 km of Bermuda between 1880 and 2019 (figure 1). The majority of these tracks originate in the North Atlantic main development region (10–20° N, 20–80° W). There is a difference in the TC genesis area between 1980 and 1999 (figure 1(b)) where the majority of tracks originate west of 50° W, whereas between 2000 and 2019 the majority of tracks originated further east just off Africa around 20–30° W (figure 1(c)). The different genesis pattern between the two periods is consistent with the all Atlantic track trend which shows a 62% increase in TC genesis (from 26 to 42 tracks) off Africa (10–20° N, 0–30° W) in the period 2000–2019 compared to 1980–1999 (figures 1(f) and (e)). In an attempt to understand the more easterly genesis in the later period, from an ocean perspective, the difference in the prevalent August, September, October (ASO) SSTs between the 1980s and 2010s was assessed figure 2 (upper). An SST warming is shown in the later period of up to 0.9 °C off the west coast of Africa at 20° N 20° W, in addition there is an $\overline{T_{50\,m}}$ warming, figure 2 (lower), off the coast of Africa (10–20° N, 10–15° W) of up to 1.1 °C, potentially related to a reduced upwelling. The SST increase results in a northward shift in the 26 °C–28 °C SST isotherms, which is consistent with increasing the potential for TC genesis in the eastern part of the Atlantic which requires a minimum SST of 26 °C (Gray 1968, Crnivec *et al* 2016, Defforge and Merlis 2017). The more easterly genesis may also be associated with changes in atmospheric variables (not explored here), such as vertical wind shear, mid-level moisture or African easterly waves (AEWs). In the Atlantic, weak vertical wind shear favourable for TC development is associated with warmer SSTs (Klotzbach 2007, Klotzbach *et al* 2018, Hallam *et al* 2019). Warmer SSTs weaken the subsidence associated with the subtropical high which consequently weakens the trade winds and associated vertical shear (Klotzbach 2007). In terms of AEW, Patricola *et al* (2018) suggest that AEW may not influence basin wide TC variability and instead AEW and TC variability may both be driven by ocean variability. Kouadio *et al* (2010) also find that a dipole in SST could contribute to enhanced continental convergence. In combination these factors may help explain the more easterly TC genesis observed.

In terms of TC intensity, figure 3(a) shows the TCs within 100 km of Bermuda from 1880 to 2019. However, the work of Vecchi and Knutson (2011) highlights that in the pre-satellite era (between 1878 and 1965) a significant upward adjustment of hurricane counts may be needed before 1965 to account for

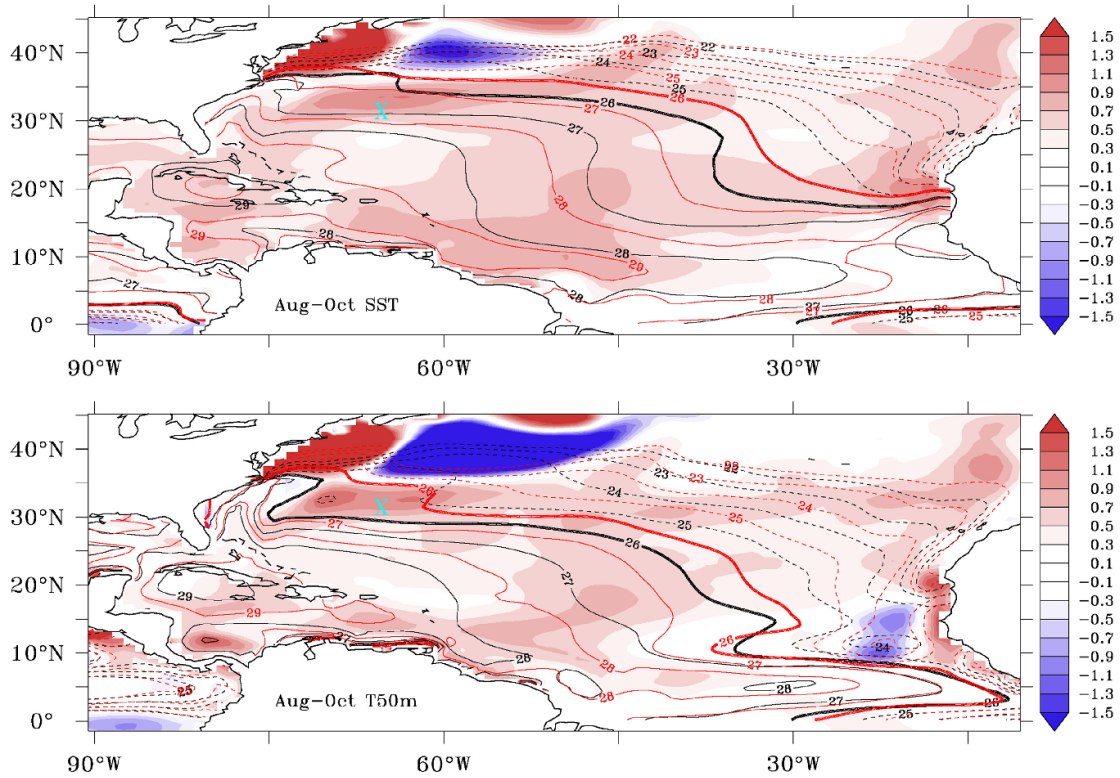

Figure 2. ASO SST difference for the period 2010–2019 compared to 1980–1990 (upper), contours show the ASO SSTs for the 1980s (black) and 2010s (red), ASO $\overline{T_{50\,\mathrm{m}}}$ temperature difference for the period 2010–2019 compared to 1980–1990 (lower) contours show the ASO $\overline{T_{50\,\mathrm{m}}}$ for the 1980s (black) and 2010s (red) X indicates the location of Bermuda.

the low density of reporting ship traffic. The research indicates that the under recording is most likely to relate to weaker TCs which are less likely to have been reported by ships (and would reduce the average intensity). More reliable is the significant increasing trend (figure 3(a)) in TC intensity between 1955 and 2019, $r = 0.4$ ($p = 0.02$) (when oceanographic data is also available from the Hydrostation S site), where an increase in MSW of 34 kts over the period is observed (5.2 kts per decade). The rate of increase in MSW between 1980 and 2019 is higher with an increase from 42 to 72 kts observed (7.7 kts per decade), $r = 0.4$ ($p = 0.01$). The box plot for the period 1955–2019 also highlights the increasing trend in intensity (figure 3(b)) where there is a significant increasing trend in the decadal Vmax median value ($r = 0.94$, $p = 0.02$) of 30 kts (4.9 kts per decade) from 33 to 63 kts (1955–2019). The Vmax trend has also been analysed comparing the Atlantic Multidecadal Oscillation (AMO) cold period (1970–1994) to the AMO warm period (1995–2019) where we find an increase of 18 kts from 45 to 63 kts (supplementary figure 1 (available online at stacks.iop.org/ERL/16/034052/mmedia)).

3.2. Hydrostation S timeseries

To understand the changes in the ASO SST and average ocean temperature ($\overline{T_{\mathrm{n}}}$) in the Bermuda area a time-series of the Hydrostation S data is used for the period 1955–2016 (figure 4). Interannual variability is evident for SST and across all the $\overline{T_{\mathrm{n}}}$ levels from 25 m to 300 m which are evaluated here. $\overline{T_{\mathrm{n}}}$ is calculated as the average temperature across the depth profile from the surface. Increasing trends are highlighted via the 5 year running means. The largest significant increase in temperature between 1955 and 2016 is seen in the ASO SST of 1.1 °C (0.17 °C per decade) $r = 0.4$ ($p < 0.01$) where there has been an increase from 26.6 °C to 27.7 °C. Significant increases are also seen in all the ASO $\overline{T_{\mathrm{n}}}$ levels with an increase between 0.5 °C and 0.7 °C (0.08 °C–0.1 °C per decade), with increases for $\overline{T_{50\,\mathrm{m}}}$ from 25.4 °C to 26 °C, $r = 0.3$ ($p < 0.01$), and for $\overline{T_{200\,\mathrm{m}}}$ 22.0 °C–22.6 °C, $r = 0.31$ ($p < 0.02$). The trends are higher if the period 1980–2016 is considered where there is a increase from 0.32 °C to 0.27 °C per decade between the surface and $\overline{T_{300\,\mathrm{m}}}$ respectively, $r = 0.4$ ($p < 0.01$). Pearson correlation coefficient was used to assess statistical significance.

GODAS reanalysis data for the North Atlantic (figure 2), also shows increasing temperatures of over 0.9 °C in the ASO SST and $\overline{T_{50\,\mathrm{m}}}$ layers between the 1980s and 2010s, in the western part of the subtropical gyre (30–35° N,60–70° W), an area characterised by clockwise circulation. The increasing temperatures led to a 1500 km ENE movement in the $\overline{T_{50\,\mathrm{m}}}$ 26 °C isotherm, from the south to the north of Bermuda, in the latter period (2010–2019). Stevens *et al* (2020)

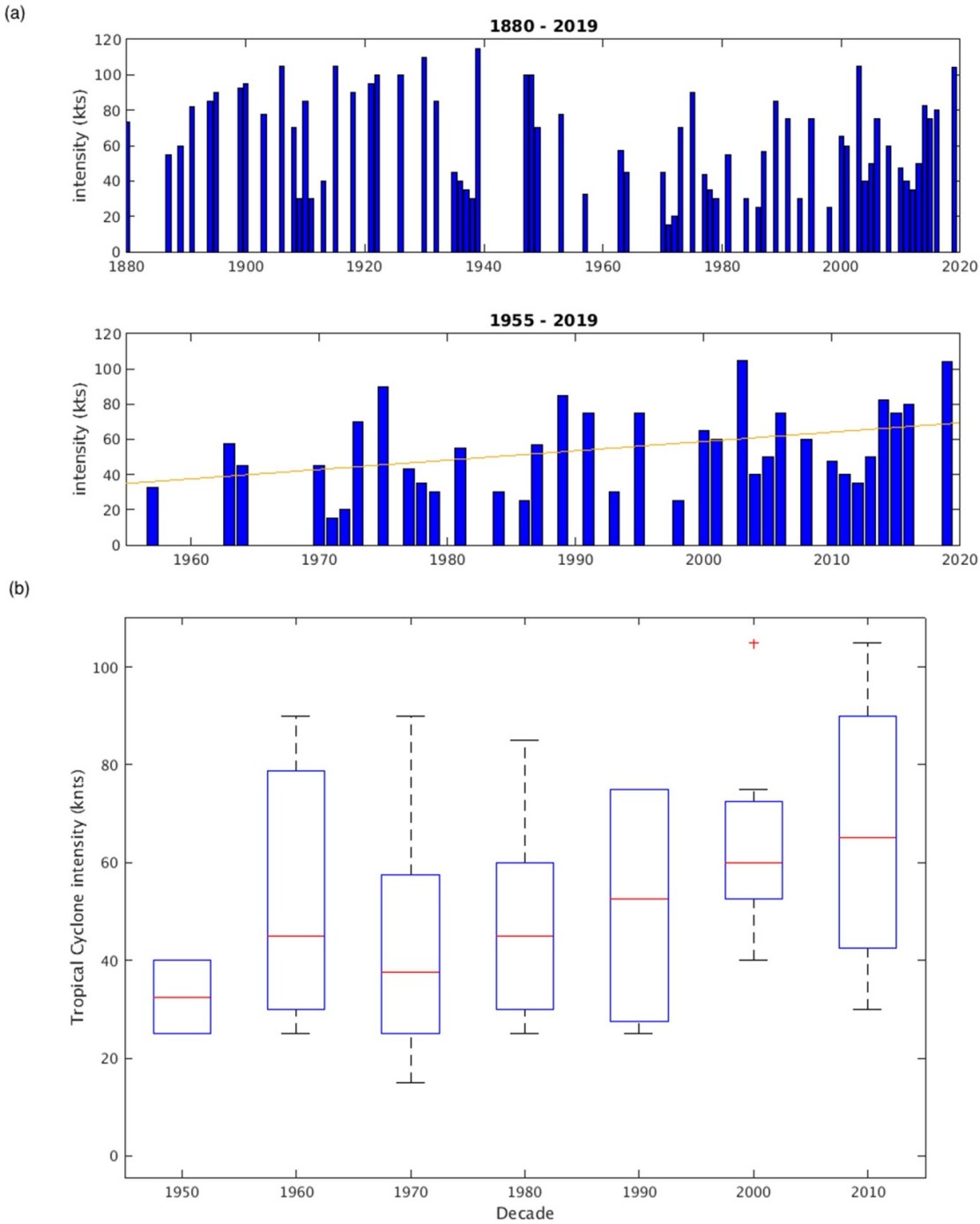

Figure 3. (a) Tropical cyclone intensity for tracks within 100 km of Bermuda for the periods 1880–2019 and 1955–2019. Orange line indicates linear trend for the period. (b) Tropical cyclone intensity box plot for tracks within 100 km of Bermuda from 1955 to 2019.

also find an increase in the OHC in the upper ocean in the western subtropical gyre between 2010 and 2018 which is anti-correlated with a reduction in subtropical mode water formation, a vertically homogeneous water mass. Around 35–40° N, 50–70° W (figure 2) there is southward shift in the 22 °C–25 °C isotherms (2010–2019), most pronounced at the $\overline{T_{50\,\mathrm{m}}}$ level, potentially associated with a shift in the inter gyre location and likely contributor to the convergence of heat observed further south.

When the ASO SST and $\overline{T_{\mathrm{n}}}$ Hydrostation S timeseries is then correlated with TC intensity in the Bermuda area (supplementary figure 2(a)) significant correlations are seen at all levels with the strongest correlation at $\overline{T_{50\,\mathrm{m}}}$, $\overline{T_{100\,\mathrm{m}}}$ and $\overline{T_{150\,\mathrm{m}}}$ $r = 0.38$ ($p < 0.01$), based on the 41 TC observations. SST has the weakest but still significant correlation at $r = 0.3$ ($p = 0.02$). These results highlight the importance of upper ocean temperature profile ($\overline{T_{\mathrm{n}}}$) to TC intensity and suggest that the increasing trend in the ASO

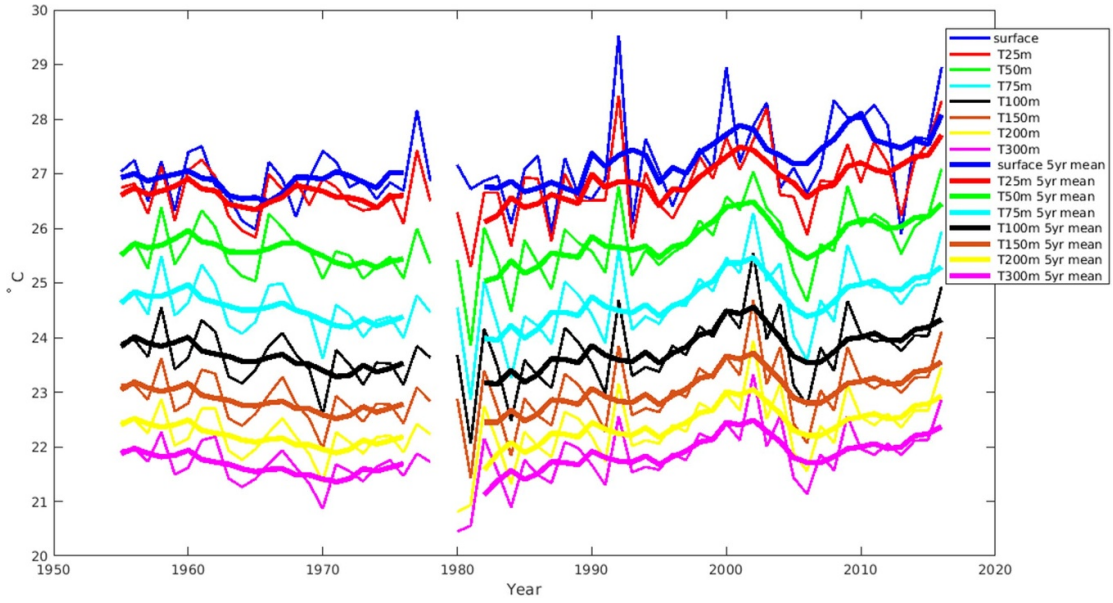

Figure 4. ASO SST and $\overline{T_n}$ time-series from the Hydrostation S site for the period 1955–2016.

SST and $\overline{T_n}$ is driving the increase in TC intensity seen (figure 3) in the subtropical area around Bermuda.

3.3. Potential intensity estimates using SST and T_n

As hurricane intensity is linked to SST and ocean thermal structure, we compare the actual maximum wind speed (Vmax) of each TC between 1955 and 2019 with SST and $\overline{T_n}$, as measured at the Hydrostation S site (figure 5) from the data immediately preceding the TC event. A significant correlation is seen between SST and Vmax (based on the Vmax for 46 TC observations), and between $\overline{T_n}$ and Vmax at depths (n) of 25 m, 50 m, 75 m (figure 5 and supplementary figure 2(b)), with the strongest significant relationship at $\overline{T_{50\,m}}$, where $r = 0.37$ ($p = 0.01$).

The results from figure 5 and supplementary figure 2 show that $\overline{T_{50\,m}}$ is most closely correlated with Vmax. This suggests that 50 m is the expected cyclone induced mixing depth resulting from vertical mixing and upwelling of cooler subsurface waters, which would be a good indication of SST during TC passage (Price 2009), and represents the SST experienced by the TC core. As an example, the ocean temperature profile preceding and after TC Paulette in September 2020 (supplementary figure 3) shows a deepening of the mixed layer depth to 50 m after the passage of the TC. In line with this, and the approach adopted by Lin *et al* (2013) who use an ocean coupling PI in their analysis in the western North Pacific, we have modified the SST PI index to create a PI index based on $\overline{T_{50\,m}}$ ($\overline{T_{50\,m}}$_PI) (3)

$$V_{\overline{T50\,m}}{}^2 = \frac{C_k}{C_D}\frac{\overline{T_{50\,m}}}{T_0}(\mathrm{CAPE}^* - \mathrm{CAPE}) \qquad (3)$$

where $\overline{T_{50\,m}}$ is the average temperature through the top 50 m ocean layer and $V_{\overline{T50\,m}}$ is the maximum wind speed. The main difference between V and $V_{\overline{T50\,m}}$ however, results from the change in computed CAPE due to the different amounts of moist entropy increase from air-sea fluxes. Replacing T_s with $\overline{T_n}$ (e.g. $\overline{T_{50\,m}}$) will change the buoyancy of air parcels, resulting in a lower V. Again in the evaluation of (3) the surface pressure at the radius of the maximum winds is calculated to provide the saturation mixing ratio necessary for CAPE* using an adapted version of equation (6) of Emanuel (1995)

$$c_p\overline{T_{50\,m}}\ln\frac{p_0}{p_m} = \frac{1}{2}V_{\overline{T50\,m}}{}^2 + \mathrm{CAPE}. \qquad (4)$$

We use equations (3) and (4) to estimate potential minimum pressure for the TCs within 100 km of Bermuda between 1955 and 2019 and compare to estimates using SST (figure 6).

The results show that when $\overline{T_{50\,m}}$ (figure 6(b)) is used to calculate the theoretical minimum pressure, the results are closer to the actual minimum pressure recorded than when SST (figure 6(a)) is used. TCs Humberto, Fabian, Nicole and Florence are labelled on figure 6 as examples. SST_PI has a correlation ($R^2 = 0.22$, slope = 0.49) for minimum pressure, $\overline{T_{50\,m}}$_PI has a higher correlation ($R^2 = 0.49$, slope = 0.6) for minimum pressure. As well as explaining 49% of the variance, the $\overline{T_{50\,m}}$_PI also reduces the TC minimum pressure difference compared to SST_PI from 27 mb to 15 mb. In all instances the minimum pressure difference between actual and predicted is lower using $\overline{T_{50\,m}}$ compared to SST (supplementary figure 4(a)). There are some instances where $\overline{T_{50\,m}}$_PI or SST_PI is very close to the actual

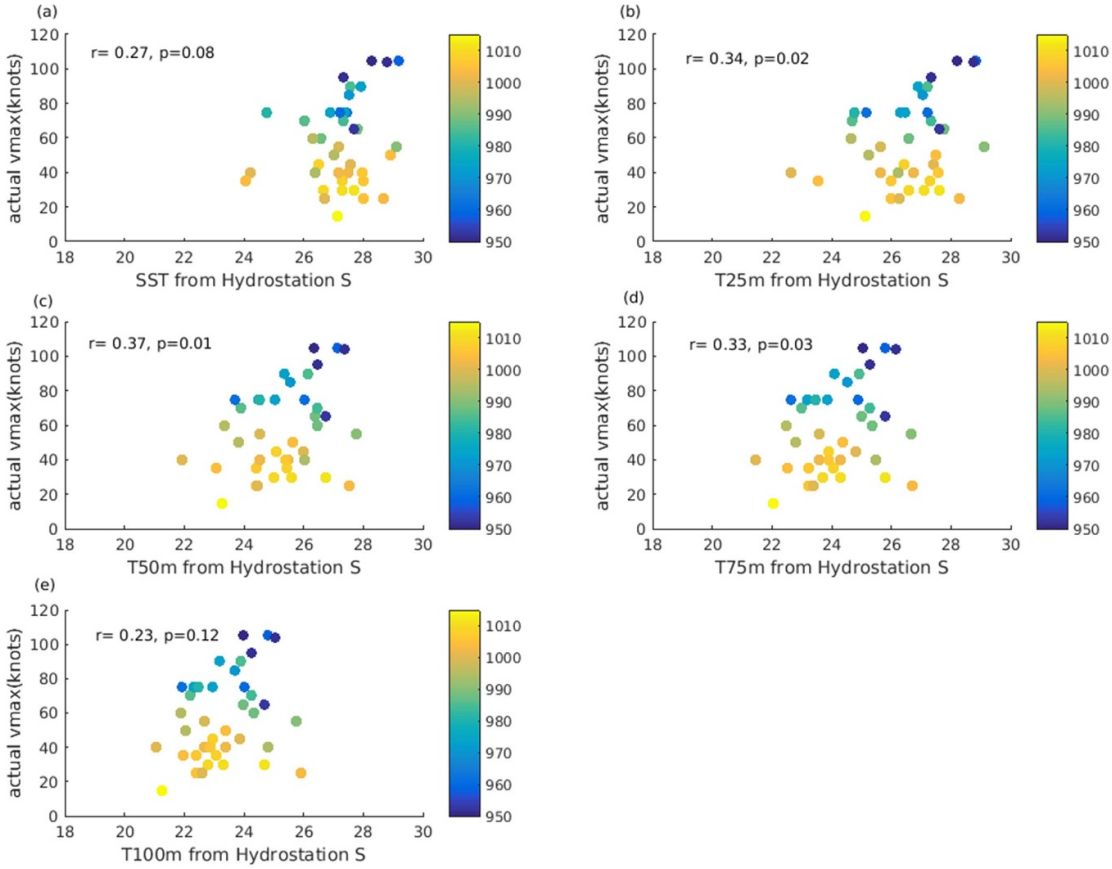

Figure 5. Tropical cyclone maximum wind (Vmax) and SST or $\overline{T_n}$, (a) SST, (b) $\overline{T_{25\,m}}$, (c) $\overline{T_{50\,m}}$, (d) $\overline{T_{75\,m}}$, (e) $\overline{T_{100\,m}}$, for tropical cyclones within a 100 km radius of Bermuda 1955–2019. Colorbar units MSLP (mb).

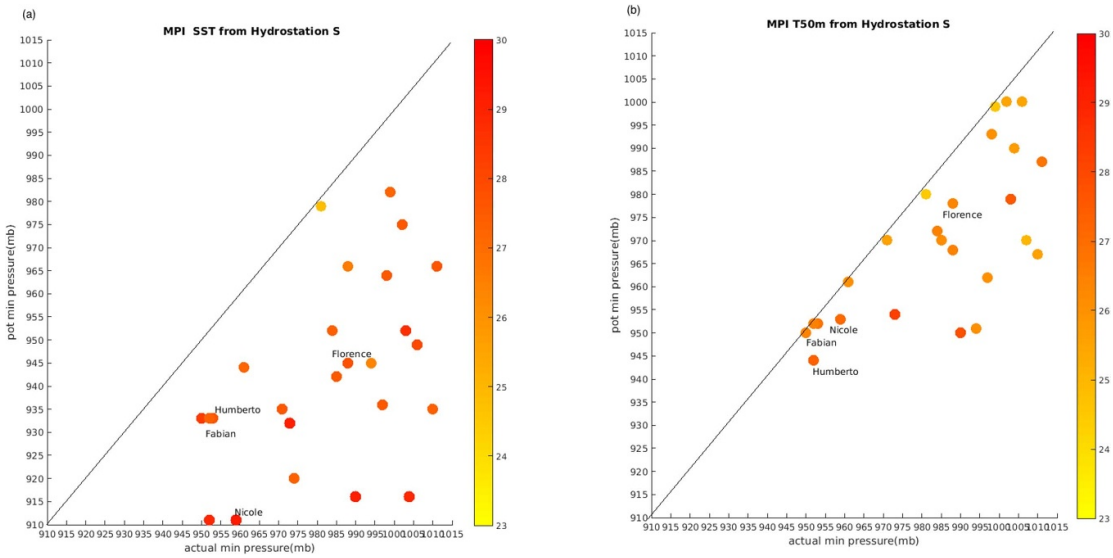

Figure 6. Tropical cyclone minimum pressure—potential intensity vs actual intensity 1955–2019 for tracks passing within 100 km radius of Bermuda. (a) SST and (b) $\overline{T_{50\,m}}$. Colorbar units temperature (°C).

PI typically where SST or $\overline{T_{50\,m}}$_is below 25.5 °C. TC reaching their PI is rare although Emanuel (2000) do find that in the Atlantic the decline of PI can be sudden, associated with sharp SST gradients, and the decline of actual storm intensity can not keep pace resulting in instances where PI can be close to or lower than actual intensity. The TCs here, where $\overline{T_{50\,m}}$_PI or SST_PI is close to the actual intensity, had passed their maximum intensity so this may explain what is observed in the results. Overall $\overline{T_{50\,m}}$_PI provides a closer prediction of actual minimum pressure which could be useful for forecasting purposes.

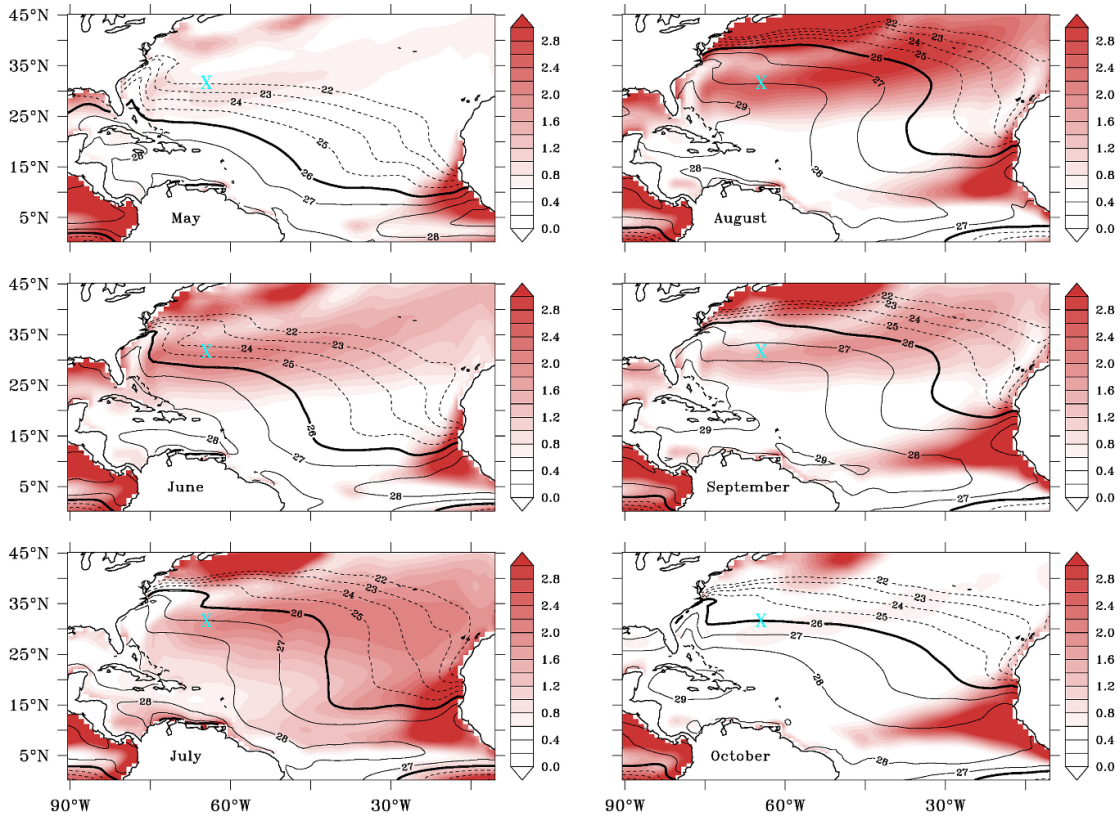

Figure 7. Monthly averaged SST (contours (°C)) and temperature difference between SST and $\overline{T_{50\,\mathrm{m}}}$ (shading (°C)) from May to October for the period 1980–2019. Location of Bermuda (X).

For the TC events between 1955 and 2019 within 100 km of Bermuda the average difference between SST and $\overline{T_{50\,\mathrm{m}}}$ was 1.8 °C with a range from 0.1 °C to 3.89 °C and a difference over 0.8 °C in 90% of TC instances. Supplementary figure 4(b) illustrates that the reduction in the potential minimum pressure difference using $\overline{T_{50\,\mathrm{m}}}$ is significantly proportional to the difference between SST and $\overline{T_{50\,\mathrm{m}}}$ ($r = 0.74$, $p < 0.01$) explaining 54% of the variance. The reduction in the minimum pressure difference observed highlights that where the mixed layer depth is shallow (<50 m), $\overline{T_{50\,\mathrm{m}}}$ can play an important role in providing a closer prediction of TC MSLP and associated MSW. Figure 7 provides further analysis and shows the temperature difference between SST and $\overline{T_{50\,\mathrm{m}}}$ between May and December across the North Atlantic (shading). In the subtropics, north of 25° N, the temperature difference is between 1 °C and 3 °C (pink and red shading) from June to September when the mixed layer depth is shallower due to surface warming. South of 25° N the temperature difference between SST and $\overline{T_{50\,\mathrm{m}}}$ is less than 1 °C from May to October, except off the west coast of Africa (10–20° N, 15–30° W) due to coastal upwelling, and during July. Using $\overline{T_{50\,\mathrm{m}}}$ to calculate TC PI where the difference between SST and $\overline{T_{50\,\mathrm{m}}}$ is more than 1 °C (figure 7 pink and red shading) could reduce the MSLP over prediction by a minimum of 15 mb (supplementary figure 4(b)).

4. Discussion and summary

In this study we have reviewed TCs in the Bermuda area from 1955 to 2019 and highlighted the more easterly genesis of tracks in the period 2000–2019 compared to 1980–1999, in line with the all Atlantic trend, and suggest, from an ocean perspective, that this is related to the increase (up to 0.9 °C) in ASO SST and $\overline{T_{50\,\mathrm{m}}}$ in the eastern Atlantic off the west coast of Africa (10–20° N, 10–20° W). In addition to the more easterly track genesis we have observed a statistically significant increase ($r = 0.94$, $p = 0.02$) in TC intensity in the Bermuda area with an increase in the Vmax median value of 30 kts (4.9 kts per decade) from 33 to 63 kts (1955–2019) and an increased trend observed for the period 1980–2019 of 7.7 kts which is in line with the increase of 8 kts per decade (1982–2009) observed over the wider Atlantic region by (Kossin *et al* 2007, 2013). We have associated the increase in TC intensity with the increasing SSTs and $\overline{T_{\mathrm{n}}}$ in the Bermuda area as measured by the Hydrostation S timeseries. The significantly increasing SST (1.1 °C) and $\overline{T_{\mathrm{n}}}$ (0.5 °C–0.7 °C) is aligned and correlated with ($r = 0.37$, $p < 0.01$), the increasing TC intensity observed over the time period 1955–2019 and consistent with other studies which suggest increasing hurricane intensity with rising ocean temperatures (Emanuel 1987, Kossin *et al* 2007, 2013, 2020). In

the early part of the record (1960–1980), however, aerosols may have suppressed the SST/OHC and associated TC intensity (Villarini and Vecchi 2013).

For the time period 1955–2019 we find TC intensity is most closely correlated with $\overline{T_{50\,\mathrm{m}}}$ in the Bermuda area and most likely represents the SST which the TC core experiences. The findings of Price (2009), Lloyd and Vecchi (2011), Huang *et al* (2015) also find that the initial upper ocean thermal profile impacts on TC intensification. In the Pacific, Lin *et al* (2013) found TC intensity most closely correlated with the ocean temperature profile through the upper 80 m, as opposed to the upper 50 m found here, possibly related to the fact that their study was conducted at lower latitude (10–30° N). Using $\overline{T_{50\,\mathrm{m}}}$ we find the TC MSLP prediction is closer to the actual value with the average prediction difference reduced by 12 mb from 27 mb to 15 mb, and proportional ($r = 0.74$, $p < 0.01$) to the temperature difference between SST and $\overline{T_{50\,\mathrm{m}}}$, a new finding here, and in accordance with Bender *et al* (2007) who found ocean coupling improved MSLP predictions. Using $\overline{T_{50\,\mathrm{m}}}$ to predict TC intensity improves TC MSLP prediction in the subtropical Bermuda area, where there is a shallow mixed layer depth from June to September, accordingly we suggest $\overline{T_{50\,\mathrm{m}}}$ would also be useful for TC prediction in the subtropical Atlantic north of 25° N and elsewhere in the tropical Atlantic when the SST/$\overline{T_{50\,\mathrm{m}}}$ temperature difference is more than 1 °C.

Data availability statement

The data that support the findings of this study are openly available at the following URL/DOI: http://bats.bios.edu/hydrostation-s-data/.

Acknowledgments

We acknowledge and thank the BATS and Hydrostation S research teams at the Bermuda Institute of Ocean Sciences who have contributed to the time-series projects since their inception. This work was supported by the Natural Environmental Research Council (NERC) (Grant Numbers NE/L002531/1), NERC project CLASS (NE/R015953/1) and the NERC programme North Atlantic Climate System: Integrated Study (ACSIS) (NE/N018044/1), the Bermuda Institute of Ocean Sciences (BIOS), with partial funding from BIOS University Programs, the Risk Prediction Initiative, and UK Associates of BIOS. PH was was supported by the Met Office Hadley Centre Climate Programme funded by BEIS and Defra.

ORCID iDs

Samantha Hallam https://orcid.org/0000-0003-3418-2554
Simon A Josey https://orcid.org/0000-0002-1683-8831
Pat Hyder https://orcid.org/0000-0002-0039-7277
Joel Hirschi https://orcid.org/0000-0003-1481-3697

References

Balaguru K, Foltz G R and Leung L R 2018 Increasing magnitude of hurricane rapid intensification in the central and Eastern Tropical Atlantic *Geophys. Res. Lett.* **45** 4238–47
Behringer D W, Ji M and Leetmaa A 1998 An improved coupled model for ENSO prediction and implications for ocean initialization. Part I: the ocean data assimilation system *Mon. Weather Rev.* **126** 1013–21
Bell K and Ray P S 2004 North Atlantic hurricanes 1977–99: surface hurricane-force wind radii *Mon. Weather Rev.* **132** 1167–89
Bender M A, Ginis I, Tuleya R, Thomas B and Marchok T 2007 The operational GFDL coupled hurricane–ocean prediction system and a summary of its performance *Mon. Weather Rev.* **135** 3965–89
Bister M and Emanuel K A 2002 Low frequency variability of tropical cyclone potential intensity 1. Interannual to interdecadal variability *J. Geophys. Res.: Atmos.* **107** ACL 26-1-ACL 26–15
Crnivec N, Smith R K and Kilroy G 2016 Dependence of tropical cyclone intensification rate on sea-surface temperature *Q. J. R. Meteorol. Soc.* **142** 1618–27
Defforge C L and Merlis T M 2017 Evaluating the evidence of a global sea surface temperature threshold for tropical cyclone genesis *J. Clim.* **30** 9133–45
Domingues R *et al* 2019 Ocean observations in support of studies and forecasts of tropical and extratropical cyclones *Frontiers Mar. Sci.* **6** 446
Emanuel K A 1987 The dependence of hurricane intensity on climate *Nature* **326** 483–5
Emanuel K A 1994 *Atmos. Convection* **580**
Emanuel K A 1995 Sensitivity of tropical cyclones to surface exchange coefficients and a revised steady-state model incorporating eye dynamics *J. Atmos. Sci.* **52** 3969–76
Emanuel K A 1999 Thermodynamic control of hurricane intensity *Nature* **401** 665
Emanuel K 2000 A statistical analysis of tropical cyclone intensity *Mon. Weather Rev.* **128** 1139–52
Emanuel K, Desautels C, Holloway C and Korty R 2004 Environmental control of tropical cyclone intensity *J. Atmos. Sci.* **61** 843–58
Goldenberg S B, Landsea C W, Mestas-nunez A M and Gray W M 2001 The recent increase in Atlantic hurricane activity: causes and implications *Science* **293** 474–9
Gray W M 1968 Global view of the origin of tropical disturbances and storms *Mon. Weather Rev.* **96** 669–700
Hallam S, Marsh R, Josey S A, Hyder P, Moat B and Hirschi J J M 2019 Ocean precursors to the extreme Atlantic 2017 hurricane season *Nat. Commun.* **10** 896
Huang P, Lin I I, Chou C and Huang R-H 2015 Change in ocean subsurface environment to suppress tropical cyclone intensification under global warming *Nat. Commun.* **6** 7188
Klotzbach P J III , Collins C J S, Bell J M, Blake M M, Eric S and Roache D 2018 The extremely active 2017 North Atlantic hurricane season *Mon. Weather Rev.* **146** 3425–43
Klotzbach P J 2007 Revised prediction of seasonal Atlantic basin tropical cyclone activity from 1 August *Weather Forecasting* **22** 937–49
Kossin J P, Knapp K R, Olander T L and Velden C S 2020 Global increase in major tropical cyclone exceedance probability over the past four decades *Proc. Natl Acad. Sci.* **117** 11975
Kossin J P, Knapp K R, Vimont D J, Murnane R J and Harper B A 2007 A globally consistent reanalysis of hurricane variability and trends *Geophys. Res. Lett.* **34**
Kossin J P, Olander T L and Knapp K R 2013 Trend analysis with a new global record of tropical cyclone intensity *J. Clim.* **26** 9960–76

Kouadio Y K, Machado L A T and Servain J 2010 Tropical Atlantic hurricanes, easterly waves, and West African mesoscale convective systems *Adv. Meteorol.* **2010** 284503

Landsea C W and Franklin J L 2013 Atlantic hurricane database uncertainty and presentation of a new database format *Mon. Weather Rev.* **141** 3576–92

Lin I I, Pun I-F and Lien C-C 2014 'Category-6' supertyphoon Haiyan in global warming hiatus: contribution from subsurface ocean warming *Geophys. Res. Lett.* **41** 8547–53

Lin I-I, Black P, Price J F, Yang C-Y, Chen S S, Lien C-C, Harr P, Chi N-H, Wu C-C and D'asaro E A 2013 An ocean coupling potential intensity index for tropical cyclones *Geophys. Res. Lett.* **40** 1878–82

Lloyd I D and Vecchi G A 2011 Observational evidence for oceanic controls on hurricane intensity *J. Clim.* **24** 1138–53

Mainelli M, Demaria M, Shay L K and Goni G 2008 Application of oceanic heat content estimation to operational forecasting of recent atlantic category 5 hurricanes *Weather Forecasting* **23** 3–16

Michaels A F and Knap A H 1996 Overview of the U.S. JGOFS Bermuda Atlantic Time-series Study and the Hydrostation S program *Deep Sea Res. Part* II **43** 157–98

Patricola C M, Saravanan R and Chang P 2018 The response of Atlantic tropical cyclones to suppression of African easterly waves *Geophys. Res. Lett.* **45** 471–9

Phillips H E and Joyce T M 2007 Bermuda's tale of two time series: Hydrostation S and BATS *J. Phys. Oceanogr.* **37** 554–71

Price J F 2009 Metrics of Hurricane-ocean interaction: vertically-integrated or vertically averaged ocean temperature? *Ocean Sci.* **5** 351–68

Shay L K, Goni G J and Black P G 2000 Effects of a warm oceanic feature on hurricane opal *Mon. Weather Rev.* **128** 1366–83

Stevens S W, Johnson R J, Maze G and Bates N R 2020 A recent decline in North Atlantic subtropical mode water formation *Nat. Clim. Change* **10** 335–41

Trenberth K E, Cheng L, Jacobs P, Zhang Y and Fasullo J 2018 Hurricane harvey links to ocean heat content and climate change adaptation *Earth's Future* **6** 730–44

Vecchi G A and Knutson T R 2011 Estimating annual numbers of Atlantic hurricanes missing from the HURDAT database (1878–1965) using ship track density *J. Clim.* **24** 1736–46

Villarini G and Vecchi G A 2013 Projected increases in North Atlantic tropical cyclone intensity from CMIP5 models *J. Clim.* **26** 3231–40

Wang Y and Wu C C 2004 Current understanding of tropical cyclone structure and intensity changes—a review *Meteorol. Atmos. Phys.* **87** 257–78

Webster P J, Holland G J, Curry J A and Chang H R 2005 Changes in tropical cyclone number, duration, and intensity in a warming environment *Science* **309** 1844–6